

Directional characteristics of cylindrical radiators with an arc-shaped acoustic screen

Pouyan Shakeri Mobarakeh · Victor Grinchenko · Babak Soltannia

Received: 20 August 2015 / Accepted: 7 May 2016 / Published online: 6 June 2016
© Springer Science+Business Media Dordrecht 2016

Abstract Directional sound radiation by a cylinder surrounded with an arc-shaped (open circular) acoustic screen is examined. The corresponding boundary problem is solved with the partial domain technique. The method of asymptotic solutions was used to verify the conditions of solving this problem using the method of simple reduction. As a result of the analysis, the quantitative characteristics of the acoustic field of the cylindrical radiator inside the arc-shaped screen were evaluated.

Keywords Asymptotic method · Directional sound radiation · Method of partial domains · Simple reduction method

Mathematics Subject Classification 76Q05

1 Introduction

Directional radiators of sound waves are widely used in various fields, for example, acoustic imaging, biomedical acoustics, and musical acoustics. The directivity of sound radiation is accomplished in two ways: either by phase matching of radiators in multicomponent systems (phased arrays) or by using different screens to obtain the desired directivity characteristics of the individual radiator.

The multifunctionality of modern radiators implies a precise control of parameters, in particular, the directional properties of their components. The effective method of controlling the directional parameters is radiator shielding. In this paper the problem of directional sound radiation by a cylinder surrounded by an arc-shaped (open circular) acoustic screen made of a sound-opaque material is considered. Cylindrical radiators, primarily owing to their

P. Shakeri Mobarakeh (✉)
Department of Theoretical and Applied Mechanics, Faculty of Mechanics and Mathematics, Taras Shevchenko National University of Kyiv, Volodymyrska Street 64, Kiev 01033, Ukraine
e-mail: pouyan.shakeri@gmail.com

V. Grinchenko
Institute of Hydromechanics, NAS of Ukraine, Zhelyabova Street 8/4, Kiev 03057, Ukraine

B. Soltannia
Department of Mechanical Engineering, University of Alberta, 4-9 Mechanical Engineering Building, Edmonton, AB T6G 2G8, Canada

processability and good strength properties, are widely employed in hydroacoustics in the design of high-power electroacoustic transducers and antennas, which are used in many applications [1–7].

The solution for the sound field generated by a shielded cylinder is constructed based on particular solutions of the Helmholtz equation for the velocity potential Φ .

The number of analytical solutions to similar applied problems is quite limited. For this reason, the approaches that extend the scope of subdomains, for which effective and instrumental solutions can be constructed for the quantitative assessment of physical field characteristics, have been devised in the last few decades. Such approaches include the so-called Schwarz algorithm [8–10], the T-matrix method [11], and the Shestopal method of solving the Riemann–Hilbert problem [12]. They are based on the decomposition of complex domains into relatively simple subdomains, for which the derived functions can be analytically represented as algebraic equations whose properties allow the method of simple reduction to be applied. In some cases, for example, the application of the T-matrix method, the derived solutions are valid only within a limited range of the domain geometry variation. This study presents a problem solution that illustrates the potentials of the new method of partial domains [13] for constructing analytical solutions for complex domains. Application of the alternative concept of the general solution opens new horizons for using the proposed approach to a wide range of problems of mathematical physics.

2 Problem statement

We examine the characteristics of sound radiation with a cylinder surrounded by an arc-shaped circular opaque layer with an acoustically soft surface (Fig. 1).

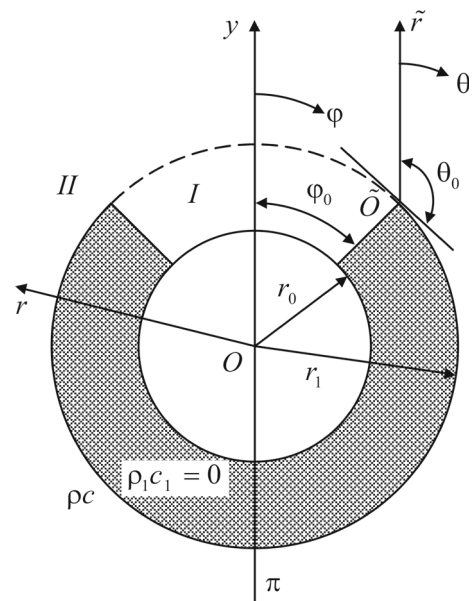
The harmonic wave field is described by the Helmholtz equation for the velocity potential [3, 14]:

$$\Delta\Phi + k^2\Phi = 0, \tag{1}$$

where $k = \omega/c$, ω is the angular frequency of harmonic waves, and c is the sound velocity. The following boundary conditions are evident from the assumption of physical layer properties:

$$\begin{aligned} \Phi &= 0; & r_0 \leq r \leq r_1, & \quad |\varphi| = \varphi_0; \\ \Phi &= 0; & r = r_1, & \quad \varphi_0 \leq |\varphi| \leq \pi. \end{aligned} \tag{2}$$

Fig. 1 Cylinder surrounded by an arc-shaped circular layer



Let a certain vibration velocity distribution $v_0 f(\varphi)$ be set on the open portion of the radiator surface. This distribution is assumed to be symmetric about the Oy axis to keep the problem from becoming too involved. Then the condition on the radiant surface takes on the following form:

$$-\frac{\partial \Phi}{\partial(kr)} = v_0 f(\varphi); \quad r = r_0, \quad 0 \leq |\varphi| \leq \varphi_0. \tag{3}$$

For the conceptual construction of the velocity potential over the domain of field existence, take the two partial domains (subdomains): $r_0 \leq r \leq r_1, |\varphi| \leq \varphi_0$ (subdomain I) and $r \geq r_1, 0 \leq |\varphi| \leq \pi$ (subdomain II).

3 Problem solution

With the preceding boundary conditions, represent the field over each of the subdomains as

$$\begin{aligned} \Phi_1 &= \sum_{q=0}^{\infty} [A_q J_{\nu_q}(kr) + B_q N_{\nu_q}(kr)] \cos \nu_q \varphi; \\ \Phi_2 &= \sum_{n=0}^{\infty} S_n H_n^{(1)}(kr) \cos n\varphi. \end{aligned} \tag{4}$$

The expression for Φ_1 obeys the Helmholtz equation at an arbitrary ν_q value. The boundary conditions can be partially met over subdomain I by the proper choice of this value. Thus, assuming

$$\nu_q = \frac{(2q + 1)\pi}{2\varphi_0}, \tag{5}$$

the first condition in (2) is satisfied at the layer edges $\varphi = \pm\varphi_0$. With such a ν_q choice, the solution for subdomain I involves two arbitrary functions on the surfaces $r = r_0$ and $r = r_1$, with $|\varphi| \leq \varphi_0$ as the Fourier series with undetermined coefficients. The Φ_2 solution for exterior subdomain $II, r \geq r_1$, satisfies the Sommerfeld condition [15] and bears a sufficient degree of functional arbitrariness to satisfy the boundary conditions on the surface $r = r_1, 0 \leq \varphi \leq 2\pi$. These properties of the Φ_1 and Φ_2 expressions create the prerequisites for fulfilling boundary conditions (2) and (3) by the appropriate choice of their arbitrary constants.

Condition (3) allows the values of the A_q and B_q coefficients to be related. Substituting the expression for Φ_1 into (3), we can easily establish that

$$B_q = \frac{L_q - A_q J'_{\nu_q}(kr_0)}{N'_{\nu_q}(kr_0)}, \tag{6}$$

where

$$L_q = -\frac{2v_0}{k\varphi_0} \int_0^{\varphi_0} f(\varphi) \cos \nu_q \varphi \, d\varphi.$$

With (6), the expression for Φ_1 is transformed into

$$\Phi_1 = \sum_{q=0}^{\infty} \left[A_q \Delta_q(kr) + L_q \frac{N_{\nu_q}(kr)}{N'_{\nu_q}(kr_0)} \right] \cos \nu_q \varphi, \tag{7}$$

where

$$\Delta_q(kr) = J_{\nu_q}(kr) - J'_{\nu_q}(kr_0)N_{\nu_q}(kr)/N'_{\nu_q}(kr_0).$$

To determine the remaining unknowns in (4), the functional equations that combine the sound field continuity condition at the subdomain boundary and the boundary condition on the surface $r = r_1$ should be applied:

$$\begin{aligned} \Phi_2 &= \begin{cases} \Phi_1 & 0 \leq |\varphi| \leq \varphi_0, \\ 0 & \varphi_0 \leq |\varphi| \leq \pi, \end{cases} \\ \frac{\partial \Phi_2}{\partial r} &= \frac{\partial \Phi_1}{\partial r} \quad 0 \leq |\varphi| \leq \varphi_0. \end{aligned} \tag{8}$$

Algebraization of functional equations (8) based on the properties of complete and orthogonal functions on the corresponding intervals leads to the following infinite system of linear algebraic equations of the second kind:

$$\begin{aligned}
 S_n H_n^{(1)}(kr_1) - \frac{1}{\delta_n} \sum_{q=0}^{\infty} A_q \Delta_q(kr_1) a_{nq} &= \frac{1}{\delta_n} \sum_{q=0}^{\infty} a_{nq} L_q N_{v_q}(kr_1) / N'_{v_q}(kr_0), \\
 A_q \Delta'_q(kr_1) - \frac{1}{\varphi_0} \sum_{n=0}^{\infty} S_n H_n^{(1)}(kr_1) a_{nq} &= -L_q N'_{v_q}(kr_1) / N'_{v_q}(kr_0),
 \end{aligned} \tag{9}$$

where

$$\delta_n = \begin{cases} 2\pi & n = 0, \\ \pi & n \neq 0, \end{cases} \quad a_{nq} = \begin{cases} \frac{2v_q(-1)^{q+1} \cos n\varphi_0}{n^2 - v_q^2} & n \neq v_q, \\ \varphi_0 & n = v_q, \end{cases}$$

$\Delta'_q(kr_1)$ is the derivative of $\Delta_q(kr)$ with respect to kr at $r = r_1$.

Thus, we must seek the values of arbitrary constants from infinite system (9) entering into Eq. (4). In this connection, the existence of the boundary problem solution is reduced to the existence proof of such a solution for system (9), which provides the convergence of infinite series for the field components everywhere over an examined domain.

The commonly used approach to studying the solvability of such systems is to prove their regularity [16]. Embarking on a study of the regularity of system (9), enter the new unknowns:

$$\tilde{S}_n = S_n H_n^{(1)}(kr_1), \quad \tilde{A}_q = A_q \Delta_q(kr_1). \tag{10}$$

With this, initial system (9) is transformed into

$$\begin{aligned}
 \tilde{S}_n \frac{H_n^{(1)}(kr_1)}{H_n^{(1)}(kr_1)} - \frac{1}{\delta_n} \sum_{q=0}^{\infty} \tilde{A}_q a_{nq} &= \frac{1}{\delta_n} \sum_{q=0}^{\infty} L_q a_{nq} N_{v_q}(kr_1) / N'_{v_q}(kr_0), \\
 \tilde{A}_q \frac{\Delta'_q(kr_1)}{\Delta_q(kr_1)} - \frac{1}{\varphi_0} \sum_{n=0}^{\infty} \tilde{S}_n a_{nq} &= -L_q N'_{v_q}(kr_1) / N'_{v_q}(kr_0).
 \end{aligned} \tag{11}$$

The complex functional dependence of the coefficients on their number in system (11) makes the analysis of its regularity more difficult. We now need to focus on the proof of the system’s quasi-regularity. In this case, it is permissible to simplify the matrix elements of the latter through the use of known asymptotic representations of the Bessel, Neumann, and Hankel functions taken as the functions of orders n and v_q . Based on those representations [17], we get

$$\frac{H_n^{(1)}(kr_1)}{H_n^{(1)}(kr_1)} = \frac{kr_1}{n}, \quad \frac{\Delta'_q(kr_1)}{\Delta_q(kr_1)} = \frac{v_q}{kr_1}, \quad \frac{N'_{v_q}(kr_1)}{N'_{v_q}(kr_0)} = \left(\frac{r_0}{r_1}\right)^{v_q+1}, \quad n, v_q \gg 1. \tag{12}$$

With (12), the following infinite system is found, which is equivalent to initial system (11) in terms of its solvability:

$$\begin{aligned}
 \tilde{S}_n^{(1)} - \frac{2n \cos^2 n\varphi_0}{\pi} \sum_{q=0}^{\infty} A_q^{(1)} \frac{1}{n^2 - v_q^2} &= \frac{2n \cos^2 n\varphi_0}{\pi kr_1} \sum_{q=0}^{\infty} L_q a_{nq} N_{v_q}(kr_1) / N'_{v_q}(kr_0), \\
 \tilde{A}_q^{(1)} - \frac{2v_q}{\varphi_0} \sum_{n=0}^{\infty} \tilde{S}_n^{(1)} \frac{1}{n^2 - v_q^2} &= -L_q \left(\frac{r_0}{r_1}\right)^{v_q+1},
 \end{aligned} \tag{13}$$

where

$$\tilde{A}_q^{(1)} = \tilde{A}_q \frac{(-1)^{q+1} v_q}{kr_1}, \quad \tilde{S}_n^{(1)} = \tilde{S}_n \cos n\varphi_0.$$

Since the coefficients $1/(n^2 - \nu_q^2)$ change their sign in each line of system (13), further analysis of the latter is quite difficult. Therefore, we proceed as follows: substitute the $\tilde{A}_q^{(1)}$ value obtained from the second equation of system (13) into the first one and determine $\tilde{S}_n^{(1)}$,

$$\tilde{S}_n^{(1)} = \frac{4n \cos^2 n\varphi_0}{\pi} \sum_{g=1}^{\infty} \tilde{S}_g^{(1)} a_{ng} + b_n, \tag{14}$$

where

$$a_{ng} = \frac{1}{\varphi_0} \sum_{q=0}^{\infty} \frac{\nu_q}{(n^2 - \nu_q^2)(g^2 - \nu_q^2)}.$$

The direct verification of fulfilling the quasi-regularity conditions of system (14) for arbitrary φ_0 values seems difficult. Therefore, we shall restrict our consideration to the specific, most unfavorable case, where $\varphi_0 = \pi$. Then the coefficients a_{ng} take on the form

$$a_{ng} = \frac{1}{\pi} \sum_{q=0}^{\infty} \frac{q + 1/2}{[(q + 1/2)^2 - n^2][(q + 1/2)^2 - g^2]}. \tag{15}$$

The general term of infinite series (15) can be represented by the following integral:

$$\frac{q + 1/2}{[(q + 1/2)^2 - n^2][(q + 1/2)^2 - g^2]} = \frac{1}{n^2 - g^2} \int_0^{\infty} [\cosh(nt) - \cosh(gt)] e^{-(q+1/2)t} dt. \tag{16}$$

Thus, we succeed in convolving the infinite series in the expression for a_{ng} and represent the coefficients of infinite system (14) as

$$\begin{aligned} a_{ng} &= \frac{1}{\pi(n^2 - g^2)} \int_0^{\infty} [\cosh(nt) - \cosh(gt)] \sum_{q=0}^{\infty} e^{-(q+1/2)t} dt \\ &= \frac{1}{2\pi(n^2 - g^2)} \int_0^{\infty} \sinh^{-1}(t/2) [\cosh(nt) - \cosh(gt)] dt. \end{aligned} \tag{17}$$

In accordance with known relations [18], the improper integrals in this expression may be represented via the special functions. Then we get

$$a_{ng} = \frac{1}{\pi(n^2 - g^2)} [\psi(n + 1/2) - \psi(g + 1/2)], \tag{18}$$

where $\psi(n + 1/2)$ and $\psi(g + 1/2)$ are the psi functions.

The psi functions [18, 19] were established to bear a constant sign. This significantly simplifies the computation of the sum of coefficient modules in system (14). With studies on quasi-regularity, for a_{ng} the following asymptotic equation may be applied:

$$a_{ng} = \frac{1}{\pi} \left[\frac{\ln(n/g)}{n^2 - g^2} - \frac{B_2}{4n^2 g^2} \right], \quad g \geq G, \tag{19}$$

which renders their value negligible as $1/n^4$ approaches unity. Here, B_2 is the Bernoulli number. G is a value of g beginning from which the asymptotic expressions may be already used for the system coefficients. To derive (19), the duplication formula and the asymptotic expansion for the psi function [19] were used.

With regard to (19), to study the quasi-regularity of (14) we have the following estimate:

$$F_n = \frac{4n}{\pi^2} \sum_{g=G}^{\infty} a_{ng} \leq \frac{4n}{\pi^2} \sum_{g=G}^{\infty} \left[\frac{\ln(n/g)}{n^2 - g^2} - \frac{B_2}{4n^2 g^2} \right] + O\left(\frac{1}{n^4}\right). \tag{20}$$

For large n values, the sum of series (20) can be calculated using the methods of summability [20]. With this

$$\sum_{g=G}^{\infty} \frac{\ln(n/g)}{n^2 - g^2} < -\frac{1}{n} \int_0^{\infty} \frac{\ln(n/g)}{1 - (n/g)^2} d(n/g)$$

for large g values, the following estimate is assumed:

$$F_n \leq 1 - \frac{1}{36n} = 1 - Q(n). \quad (21)$$

Thus, system (14) is quasi-regular. The existence of the bounded solution is now reduced to a comparison of descending orders of the function $Q(n)$ and free terms in (14). Behavioral analysis of the free terms in (14) shows that they decrease as $1/n^2$, i.e., more rapidly than the function $Q(n)$ in (21). It is indicative of the possibility of applying the method of simple reduction for finding the approximate solution of (14) and, thus, system (11).

Based on the existence of the bounded solution for system (11), it can be demonstrated that the infinite series in (4) and corresponding series for the vibration velocity converge in all the points of partial domains. This suggests the existence of the boundary problem solution in the adopted form. Nevertheless, in terms of actually finding the solution and further interpreting quantitatively the general formulas for the physical values that characterize the field, the regularity of the infinite system practically has little to offer. More comprehensive information on the potentials of the approach to the solution of boundary problems in complex domains can be gained from an analysis of the examined physical fields. In this connection, we analyze briefly the stages of solving the problem of cylinder sound radiation through an arc-shaped layer that preceded the derivation of infinite system (11).

To arrive at an unambiguous solution of the examined problem, the following conditions should be fulfilled: (1) boundary conditions on the cylinder and layer surfaces, (2) continuity conditions for the field components at the interface of partial domains, (3) radiation conditions at infinity, and (4) quite specific type of the vibration velocity in approaching the angular points (edges).

With respect to meeting the boundary conditions, v_q can be uniquely determined and A_q and B_q values be related. The requirement of satisfying the radiation condition at infinity specified the form of radial functions in the expression for Φ_2 . The satisfaction of mean-square continuity conditions resulted in an infinite system of algebraic equations for the coefficients of infinite series in Φ_1 and Φ_2 .

This analysis makes it clear that the fourth condition has not been explicitly applied anywhere.

With the preceding method of representing the sound field, the existence of solutions with different vibration velocity singularities in the angular points may lead to the existence of several solutions for infinite system (11). In this case, the algorithm for reducing the infinite system to a finite one should offer the finding of a desired solution, i.e., one that is consistent with physically valid velocity field characteristics in the angular points.

A knowledge of the sound field characteristics near the angular points allows us to apply a theorem known in Fourier series theory [21]: if $f(x) = \sum_{n=0}^{\infty} a_n \cos nx$ and $f(x) \sim 1/x^\alpha (x \rightarrow 0)$, then $a_n \sim 1/n^{1-\alpha} (n \rightarrow \infty)$. Just this allows for significant improvement in the procedure for solving infinite systems.

In the vicinity of the right angle formed by the surface $r = r_1$ and plane $\varphi = \varphi_0$, the vibration velocity exhibits a singularity of the $1/\tilde{r}^{1/3}$ type, where \tilde{r} is the distance from the angle vertex. In this connection, the distribution of the radial vibration velocity component over the surface $r = r_1$ can be given as

$$v_r(\varphi) = \begin{cases} \frac{-ks}{(\cos \varphi - \cos \varphi_0)^{1/3}} + v_1(\varphi) & 0 \leq \varphi \leq \varphi_0, \\ -\frac{ks}{(\cos \varphi_0 - \cos \varphi)^{1/3}} + v_2(\varphi) & \varphi_0 \leq \varphi \leq \pi, \end{cases} \quad (22)$$

where s is a certain constant, and $v_1(\varphi)$ and $v_2(\varphi)$ are regular functions. The principal terms in (22) examined on the complete interval $0 \leq \varphi \leq \pi$ can be expressed as the Fourier series

$$v_r(\varphi) = \sum_{n=0}^{\infty} a_n \cos n\varphi. \quad (23)$$

Thus, the principal, slowest decreasing part of the coefficients a_n is defined as

$$\tilde{a}_n = \frac{2}{\pi} \int_0^{\varphi_0} \frac{ks \cos n\varphi}{(\cos \varphi - \cos \varphi_0)^{1/3}} d\varphi + \frac{2}{\pi} \int_{\varphi_0}^{\pi} \frac{ks \cos n\varphi}{(\cos \varphi_0 - \cos \varphi)^{1/3}} d\varphi. \tag{24}$$

With the integral representations for the Legendre functions of the first and second kinds [22], it is easy to show that

$$\tilde{a}_n = ks \left[P_{n-1/2}^{-1/6}(\cos \varphi_0) + \frac{2}{\pi} \frac{(n + 1/3)}{(n + 2/3)} Q_{n-1/2}^{1/6}(\cos \varphi_0) \right]. \tag{25}$$

The asymptotic representations of the Legendre functions for large indices [17,22] allow us to obtain the following asymptotic estimates for the coefficients of series (23):

$$\tilde{a}_n = A \frac{\cos n\varphi_0}{n^{2/3}}, \quad n \gg 1. \tag{26}$$

Based on the foregoing reasoning, one notices that relation (26) defines behavior with growth in a number of the unknowns \tilde{S}_n in system (11). If one makes use of only the first part of the expression (which corresponds to $0 \leq \varphi \leq \varphi_0$) for $\nu_r(\varphi)$ in (22) and develops it as series in the complete system of the functions $\cos \nu_q \varphi$ on the interval $0 \leq \varphi \leq \varphi_0$, then the estimate of the asymptotic behavior of the unknowns \tilde{A}_q in system (11) can be obtained:

$$\tilde{A}_q^{(0)} = B \frac{(-1)^{q+1}}{\nu_q^{5/3}}, \quad q \gg 1. \tag{27}$$

Relations (26) and (27) define the assumed asymptotic properties of the unknowns in system (11), which were obtained from the analysis of the edge conditions necessary for the existence of the unique solution to the boundary problem. To support the existence of such a solution of infinite system (11), the consistency of asymptotic estimates (26) and (27) can be verified with the same relations of the infinite system.

From the properties of the unknowns \tilde{A}_q , determine the asymptotic properties \tilde{S}_n . At large n indices from the first equation of system (11), the following representation takes place:

$$\tilde{S}_n^{(0)} \frac{kr_1}{n} = \frac{1}{\pi} \sum_{q=0}^{\infty} \tilde{A}_q a_{nq} + O(n^{-2}), \quad n \gg 1. \tag{28}$$

Estimate the sum in the latter expression,

$$\begin{aligned} J &= \frac{1}{\pi} \sum_{q=0}^{\infty} \tilde{A}_q a_{nq} = \frac{1}{\pi} \sum_{q=0}^{\infty} \tilde{A}_q^{(0)} a_{nq} + \frac{1}{\pi} \left[\sum_{q=0}^{Q-1} \tilde{A}_q a_{nq} - \sum_{q=0}^{Q-1} \tilde{A}_q^{(0)} a_{nq} \right] \\ &= \frac{1}{\pi} \sum_{q=0}^{\infty} \tilde{A}_q^{(0)} a_{nq} + O(n^{-2}), \end{aligned} \tag{29}$$

where Q is the minimum value of index q , for which the substitution of the Bessel and Neumann functions with their asymptotic representations is held valid, and $\tilde{A}_q^{(0)}$ is the asymptotic value of the coefficients \tilde{A}_q at $q \gg 1$.

With (27), we get

$$J = B \cos n\varphi_0 \sum_{q=0}^{\infty} \frac{1}{\nu_q^{2/3} (n^2 - \nu_q^2)}. \tag{30}$$

The sum in this expression can easily be estimated with the method of summability of infinite series [20]:

$$\sum_{q=0}^{\infty} \frac{1}{\nu_q^{2/3} (n^2 - \nu_q^2)} \leq \frac{\varphi_0}{\pi n^{5/3}} \int_0^{\varphi_0} \frac{dx}{x^{2/3} (1 - x^2)} = \frac{\varphi_0}{\pi n^{5/3}} \cdot \frac{\pi}{2} \cot \frac{\pi}{6} = \frac{\varphi_0 \sqrt{3}}{2n^{5/3}}. \tag{31}$$

Thus, with an accuracy to $O(n^{-5/3})$, we have

$$J = B \frac{\varphi_0 \sqrt{3} \cos n\varphi_0}{2 n^{5/3}}. \tag{32}$$

With estimates (32) from (28), we finally obtain

$$\tilde{S}_n^{(0)} = B \frac{\varphi_0 \sqrt{3} \cos n\varphi_0}{2kr_1 n^{2/3}}. \tag{33}$$

The second relation in system (11) used for similar calculations permits of establishing the total consistency of estimates (26) and (27), derived from general considerations, with the properties of the coefficients in system (11).

The solution algorithm for system (11) should ensure such a solution whose asymptotic properties are determined by relations (26) and (27). In this connection, for the finite system with the N and Q unknowns, we assume

$$\begin{aligned} \tilde{S}_n &= \tilde{S}_N \frac{\cos n\varphi_0}{\cos N\varphi_0}, \quad n \gg N, \\ \tilde{A}_q &= \tilde{A}_N \left(\frac{v_Q}{v_q}\right)^{5/3} (-1)^{q-Q}, \quad q \gg Q. \end{aligned} \tag{34}$$

With relations (34), system (11) can be put in the form

$$\begin{aligned} \tilde{S}_n \frac{H_n^{(1)}(kr_1)}{\tilde{H}_n^{(1)}(kr_1)} - \frac{1}{\delta_n} \sum_{q=0}^{Q-1} \tilde{A}_q a_{nq} - \frac{\tilde{A}_Q}{\delta_n} \sum_{q=Q}^{\infty} \left(\frac{v_Q}{v_q}\right)^{5/3} a_{nq} &= \frac{1}{\delta_n} \sum_{q=0}^{\infty} L_q a_{nq} \frac{N_{v_q}(kr_1)}{N'_{v_q}(kr_1)}, \\ \tilde{A}_q \frac{\Delta'_q(kr_1)}{\Delta_q(kr_1)} - \frac{1}{\varphi_0} \sum_{n=0}^{N-1} \tilde{S}_n a_{nq} - \frac{\tilde{S}_N}{\varphi_0} \sum_{n=N}^{\infty} \left(\frac{N}{n}\right)^{2/3} \frac{\cos n\varphi_0}{\cos N\varphi_0} a_{nq} &= L_q \frac{N'_{v_q}(kr_1)}{N'_{v_q}(kr_0)}. \end{aligned} \tag{35}$$

The foregoing data on a decrease in the coefficients of infinite series, which represent the sound fields in the partial domains, can be used to estimate the rates of their convergence. Thus, to study the characteristics of the far-zone field, one should apparently proceed from the following representation:

$$\Phi_2 \approx \Phi_0 \sum_{n=0}^{\infty} \tilde{S}_n \cos n\varphi \quad \Phi_0 = \left(\frac{2}{\pi kr_1}\right)^{1/2} e^{i(kr-\pi/4)}. \tag{36}$$

With (26), we find for \tilde{S}_n

$$\tilde{S}_n \approx \text{const} \frac{(kr_1)^n \cos n\varphi_0 e^{in\pi/2}}{n^{2/3}(n-1)!}, \quad n \gg 1. \tag{37}$$

The Fourier series (36) with the coefficients \tilde{S}_n for the cylinder with a surrounding layer of not very large diameter-to-wavelength ratios converges very fast. This suggests that for a quantitative description of the far-zone field it would be sufficient to know the values of several first coefficients \tilde{S}_n . A similar estimation can be performed for the near-zone field. With Eqs. (7) and (10), the velocity potential over domain I is given by the following series:

$$\Phi_1 = \sum_{q=0}^{\infty} \left[A_q \frac{\Delta_q(kr)}{\Delta_q(kr_1)} + L_q \frac{N_{v_q}(kr)}{N'_{v_q}(kr_0)} \right] \cos v_q \varphi. \tag{38}$$

Based on the asymptotic properties of the coefficients \tilde{A}_q (27), we notice that the convergence of series (38) at $r = r_0$ is the same as that of the Fourier series with the coefficients

$$\frac{2}{\pi} \frac{(-1)^{q+1}}{v_q^{5/3}} \left(\frac{r_0}{r_1}\right)^{v_q} + \frac{(-1)^{q+1} kr_0}{v_q^2}. \tag{39}$$

The analysis of convergence of infinite series shows that for quantitative estimation of engineering characteristics of a sound field, one need only have knowledge of several first coefficients in corresponding series. This is evidence that in a number of cases, system (11) can be solved with the method of simple reduction. The potentials of such an approach are corroborated by the additional quantitative data given in what follows. Noteworthy is that the application of the preceding method is acceptable if the following conditions are fulfilled: (1) with an increase in the number of unknowns in system (11), its solution would tend to that of a system with required asymptotic properties; (2) values of the unknowns with small numbers would be determined quite accurately with a comparatively small number of equations in a system obtained by the reduction of system (11). These conditions can be verified by comparing the solution results of system (11), gained by simple reduction, and of system (35), constructed with the asymptotic properties of unknowns (improved reduction method).

4 Results and discussion

4.1 Computational results

Table 1 lists several \tilde{S}_n values computed at $N = 6$ and $Q = 6$ with the assumption of $kr_0 = 1.6$, $kr_1 = 2.89$, $\varphi_0 = \pi/2$, and $f(\varphi) = 1$. The second column of Table 1 corresponds to the method of the simple reduction of system (11), and the third one contains the result for system (35), obtained using the improved reduction method.

The data in Table 1 are evidence in favor of the following assertions. First, the method of simple reduction used for finding the unknowns in system (11) actually gives the solution with their asymptotic properties corresponding to the essentials of the problem. Second, for deriving reliable values of several first unknowns, it suffices to consider a system holding about twice as many unknowns as those necessary for obtaining quantitative estimates of the field characteristics. The latter assertion is also corroborated by computational results for different geometric and wave parameters of a cylindrical radiator with an arc-shaped layer, as well as by data available in the literature [23,24].

Thus, the analysis gives grounds for inferring that the far-zone field and radiation impedance can be evaluated to a good approximation from the solution results of infinite system (11) obtained by the method of simple reduction. However, to study the local field characteristics, especially on the surface $r = r_1$, where the series defining pressure and vibration velocity feature the slowest convergence, system (35) is used, employing known methods of improving the convergence of Fourier series [16].

Table 1 Computed \tilde{S}_n values obtained using simple and improved reduction methods

n	\tilde{S}_n	
	Simple reduction	Improved reduction
0	$-1.397148 \times 10^{-1} + i 4.193470 \times 10^{-2}$	$-1.379932 \times 10^{-1} + i 4.343100 \times 10^{-2}$
1	$-3.615388 \times 10^{-2} + i 2.376839 \times 10^{-1}$	$-3.345683 \times 10^{-2} - i 2.346520 \times 10^{-1}$
2	$-1.397027 \times 10^{-1} - i 3.035603 \times 10^{-2}$	$-1.410888 \times 10^{-1} - i 2.456649 \times 10^{-2}$
3	$-5.670435 \times 10^{-4} + i 2.611376 \times 10^{-2}$	$-5.770254 \times 10^{-4} + i 2.671194 \times 10^{-2}$
4	$-2.328268 \times 10^{-2} + i 4.271593 \times 10^{-3}$	$-2.000019 \times 10^{-2} + i 4.205960 \times 10^{-3}$
5	$-3.206226 \times 10^{-5} - i 3.395070 \times 10^{-3}$	$-3.404527 \times 10^{-6} - i 3.342761 \times 10^{-3}$
6	$-1.540533 \times 10^{-2} + i 3.235455 \times 10^{-3}$	$-1.650261 \times 10^{-2} + i 7.595264 \times 10^{-3}$
7	$-7.250446 \times 10^{-8} + i 7.387453 \times 10^{-4}$	$-6.120918 \times 10^{-7} + i 7.417587 \times 10^{-4}$
8	$-1.115143 \times 10^{-2} - i 6.101197 \times 10^{-3}$	$-6.327824 \times 10^{-3} - i 8.438423 \times 10^{-4}$
9	$-2.862725 \times 10^{-7} - i 1.719243 \times 10^{-4}$	$-1.085472 \times 10^{-6} - i 1.706887 \times 10^{-4}$
10	$-8.814035 \times 10^{-3} + i 7.677106 \times 10^{-3}$	$-1.392445 \times 10^{-2} + i 2.575785 \times 10^{-2}$
11	$-1.021961 \times 10^{-7} + i 4.224494 \times 10^{-5}$	$-5.933418 \times 10^{-8} + i 4.245868 \times 10^{-5}$

4.2 Directional characteristics and radiation impedance of a cylinder surrounded by an arc-shaped circular layer

The computational results from the previous section allow us to proceed with a study of the quantitative characteristics of the sound field of a cylindrical radiator surrounded by an arc-shaped circular layer. Our prime interest is with the far-zone field of the radiator, which is conveniently characterized by the directional pattern and directivity [25]. The normalized directional pattern $R(\varphi)$ can easily be plotted on the basis of relation (4) defining the external field of the radiator, applying the asymptotic representation of the Hankel function for the large argument values:

$$R(\varphi) = \frac{\sum_{n=0}^N S_n e^{in\pi/2} \cos n\varphi}{\sum_{n=0}^N S_n e^{in\pi/2} \cos n\varphi_1}, \quad (40)$$

where N is dependent on the order of an actually solved finite system, and φ_1 is the direction relative to which normalization is done (hereinafter $\varphi_1 = 0$).

In the strict sense, the directivity for the plane problem cannot be determined. Nevertheless, the value

$$K = \pi \left[\int_0^\pi R^2(\varphi) d\varphi \right]^{-1} \quad (41)$$

can be used; it is treated in [25] as the directivity per unit height of the cylindrical radiator and, in fact, characterizes the directional action only in the plane normal to its longitudinal axis.

Far- and near-zone field characteristics will be examined with the numerical solution of system (11). The order of truncation of this system was chosen on the basis of the foregoing analysis of series convergence.

For the data given in what follows, the number of unknowns S_n was 12, and that of the unknowns A_q was defined from the condition $\nu_q \approx 12$. In all the calculations, the vibration velocity was assumed to be uniformly distributed over the cylinder surface, i.e., $f(\varphi) = \text{const}$.

Giving a general idea of the angular distribution of sound energy radiated by the cylinder in the far-zone field, one notices that it exhibits a clearly defined nonuniformity. The directional patterns for several angle φ_0 values are shown in Fig. 2. As is seen, most of the sound energy is radiated to the front half-space $|\varphi| \leq \pi/2$, while only a small amount of energy falls on the rear one.

The directional properties of an examined radiator will be further analyzed in more detail. The width of the main directional lobe $\varphi_{0,7}$, determined from a 0.7 level, versus the maximum value $R(\varphi)$ and the directivity K versus angle $2\varphi_0$ plots are given in Fig. 3. As follows from those data, at a relatively large thickness-to-wavelength ratio of the layer, there is a certain angle φ_0 such that the major lobe width is at a minimum, while the directivity is at its maximum. These patterns are attributable to the following reasons. At sufficiently minor φ_0 , the aperture

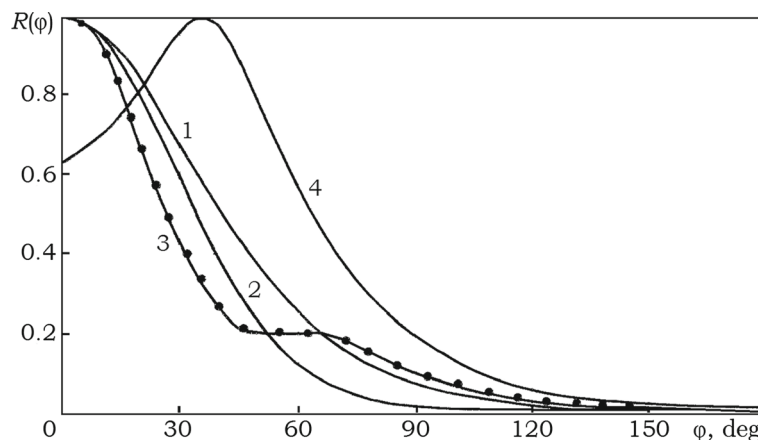


Fig. 2 Directional patterns for $kr_0 = 4.52$ and $kr_1 = 6.9$; curves 1, 2, 3, and 4 correspond to $\varphi_0 = \pi/6, \pi/4, \pi/3$, and $\pi/2$, respectively

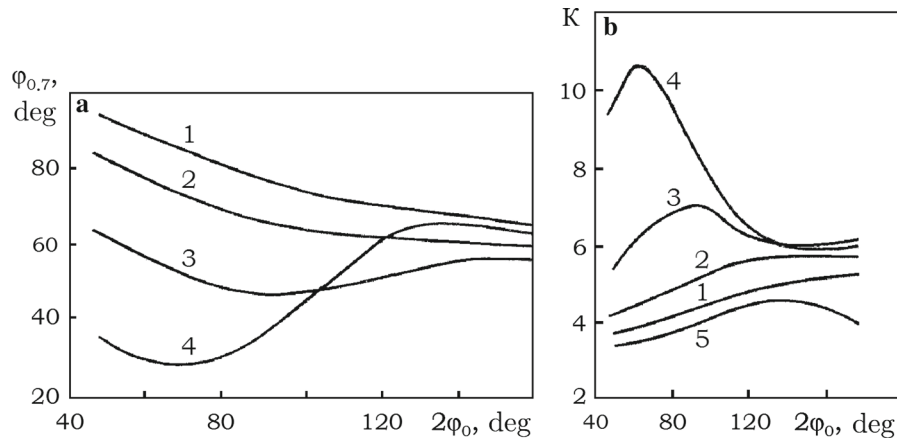


Fig. 3 Width of major **a** directional lobe and **b** directivity versus angle $2\varphi_0$ for $kr_0 = 2.26$; curves 1, 2, 3, and 4 correspond to $kr_1 = 2.89, 4.14, 6.18,$ and $14.82,$ respectively; curve 5 corresponds to the case $(r_1 - r_0)/\lambda \leq 0.1$

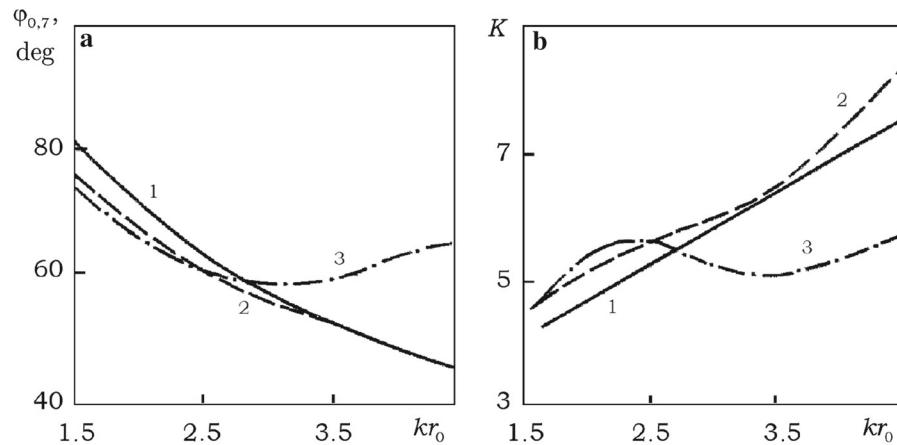


Fig. 4 Values **a** $\varphi_{0.7}$ and **b** K versus frequency response curves for $r_1/r_0 = 1.8$; curves 1, 2, and 3 correspond to angles $\varphi_0 = \pi/4, \pi/3,$ and $\pi/2$

diameter-to-wavelength ratio (by *aperture* is meant the distance between the points $r = r_1, \varphi = \pm\varphi_0$) is small, which dictates a high $\varphi_{0.7}$ value and a low K value. With an increase in φ_0 , the aperture/wavelength ratio and radiator directionality grow, which appears as a decrease in $\varphi_{0.7}$ and an increase in K . However, this process continues up to a certain limit where phase distortions caused by the cylindrical wave front in the aperture reach a significant value. This process alone retards a further narrowing of the major lobe, and at sufficiently large values even reverses, viz. the major lobe starts to widen again and, in some cases, bifurcate (e.g., curve 4 in Fig. 2). It may be expected that a decrease in the layer thickness-to-wavelength ratio (at a fixed kr_0 value) should give rise to a certain stabilization of the radiator directional properties. Actually, the calculations demonstrate that in the $(r_1 - r_0)/\lambda \leq 0.1$ range, either the directional pattern or the directivity does not practically change (curve 5 in Fig. 3b).

Here, we dwell on the relations between the major characteristics of a cylindrical radiator with an arc-shaped circular layer and frequency response. A set of $\varphi_{0.7}$ and K versus frequency curves at different φ_0 values is presented in Fig. 4. These data reveal the existence of angles such that $\varphi_{0.7}$ and K values are practically frequency-independent. Thus, an examined radiator with certain geometrical parameters features the retention of the directional lobe position over a rather wide frequency band.

It is worth noting the limiting case where $\varphi_0 = \pi$ and the circular layer degenerates into a belt whose thickness tends to zero. In this case, the effective radiation of sound energy occurs over a wide range of angles (approximately

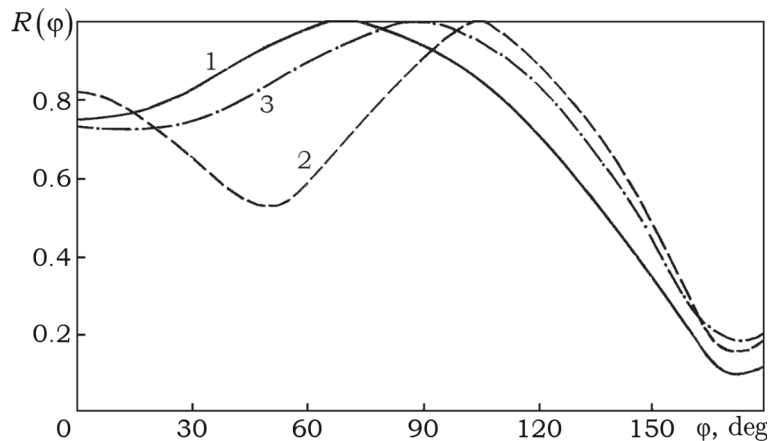


Fig. 5 Directional patterns for $\varphi_0 = \pi$ and $kr_1 = 6.18$; curves 1, 2, and 3 correspond to $kr_0 = 1.57, 2.26,$ and 3.14

from 0° to 120°), and only in the range of larger angles does the field intensity start to decrease rapidly. Several typical directional patterns are shown in Fig. 5. These data clearly demonstrate the form of the directional pattern for the aforementioned specific case, as well as the efficiency of the belt shape in the suppression of the rear-side cylinder radiation (back lobe). In hydroacoustics, radiations with such directional properties are usually termed *radiators with a sector-shaped pattern*, which find extensive practical applications [25].

We now turn to the analysis of radiation impedance characteristics of a cylinder in the arc-shaped circular layer. With the general definition of radiation impedance and the expression for the sound field in subdomain I , the radiation impedance per unit height of the cylinder can be presented in the following form, conventionally used in acoustics:

$$Z = \rho c \bar{S} (R + iX), \quad (42)$$

where $\bar{S} = 2r_0\varphi_0$ is the radiant surface area of the radiator per unit height,

$$R = \frac{1}{\pi r_0} \sum_{q=0}^{\infty} \Im(A_q) \frac{L_q}{N'_{v_q}(kr_0)},$$

$$X = -\frac{1}{2r_0} \sum_{q=0}^{\infty} \left[\frac{2}{\pi} \Re(A_q) + r_0 L_q N_{v_q}(kr_0) \right] \frac{L_q}{N'_{v_q}(kr_0)}.$$

The frequency dependence of radiation impedance components at different φ_0 angles is plotted in Fig. 6. Analyzing the frequency-dependent run of the curves, the following effects may be pointed out: with a decrease in the angle φ_0 , the impedance components reach relatively large values at high kr_0 values, while R and X values within the extreme curve sections increase with a decrease in the φ_0 angle and growth of r_1/r_0 . The r_1/r_0 effect was evaluated by comparing the data (Fig. 6) and calculation results for $r_1/r_0 = 1.1$. In this case, the slope of the curves characterising the R variation with kr_0 growth declines with a decrease in the general level of the radiant system reactivity.

Thus, the cylinder in an arc-shaped circular layer can effectively radiate sound energy only at certain frequencies depending on the φ_0 value. Below those frequencies, it quickly decreases in efficiency, with the rate of this decrease being determined by the r_1/r_0 ratio.

Assuming $r_1 \rightarrow \infty$, we arrive at the case [26] of studying the radiation impedance of a cylinder mounted on an infinite fluid wedge with acoustically soft edges. This is equivalent to the case of the infinite thickness of an arc-shaped circular layer. Comparing the results [26] and the data (Fig. 6), it may be inferred that R and X values in both cases coincide within graphical accuracy.

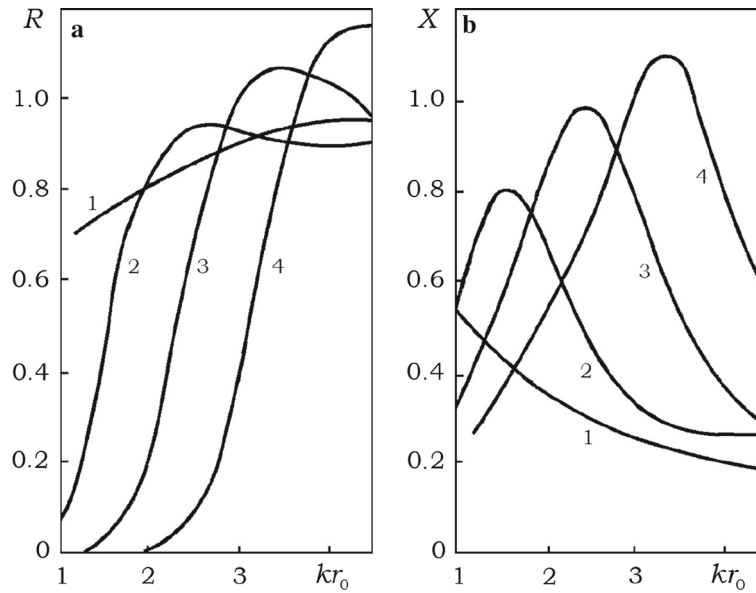


Fig. 6 Radiation impedance of cylinder within arc-shaped layer for $r_1/r_0 = 2.5$; panels **a** and **b** show real and imaginary parts, respectively; curves 1, 2, 3, and 4 correspond to $\varphi_0 = \pi/2, \pi/4, \pi/6,$ and $\pi/8$, respectively

5 Conclusions

Based on the foregoing analysis, the following conclusions can be drawn.

1. An acoustically soft arc-shaped layer makes it possible to effectively control the directional characteristics of a cylindrical radiator and its directivity. The proper choice of layer parameters can stabilize the directional pattern over a certain frequency range, i.e., provide a required frequency response of the radiator. At $r_1/r_0 \geq 2.5$, the diffraction effects caused by the finite layer thickness do not significantly affect the impedance.
2. The results give insight into the major characteristics of cylindrical radiators with arc-shaped circular screens, which can be instrumental in the design of sonar antennas and other acoustic equipment.

Acknowledgements The authors wish to acknowledge the financial support of the Natural Sciences and Engineering Research Council of Canada (NSERC) and Alberta Innovate Technology Futures (AITF). Finally, we thank the editors and reviewers for their constructive comments and suggestions, which helped in improving the quality of the final manuscript.

References

1. Beranek LL, Mellow TJ (2012) Acoustics: sound fields and transducers. Academic Press, Amsterdam
2. Crocker MJ (ed) (1997) Encyclopedia of acoustics. Wiley, New York
3. Grinchenko VT, Vovk IV, Matsipura VT (2007) Foundations of acoustics. Naukova Dumka, Kiev (in Ukrainian)
4. Sharapov V, Sotula Zh, Kunickaya L (2014) Piezo-electric electro-acoustic transducers. Springer, Heidelberg
5. Sharapov V (2011) Piezoceramic sensors. Springer, Heidelberg
6. Glazanov VE (1986) Shielding of hydro-acoustic antennas. Sudostroenie, Leningrad (in Russian)
7. Shenderov EL (1989) Radiation and scattering of sound. Sudostroenie, Leningrad (in Russian)
8. Toselli A, Widlund O (2005) Domain decomposition methods—algorithms and theory. Springer, Berlin
9. Mathew TPA (2008) Domain decomposition methods for the numerical solution of partial differential equations. Springer, Berlin
10. Langtan HP, Tveito A (eds) (2003) Advanced topics in computational partial differential equations. Springer, Berlin
11. Waterman PC (1976) Matrix theory of elastic wave scattering. J Acoust Soc Am 60(3):567–580
12. Shestopal VP (1971) Method of the Ryman-Hilbert problem in the theory of diffraction and propagation of electromagnetic waves. Kharkov University, Kharkov (in Russian)

13. Shakeri Mobarakeh P, Grinchenko VT (2015) Construction method of analytical solutions to the mathematical physics boundary problems for non-canonical domains. *Rep Math Phys* 75(3):417–434
14. Morse PM, Feshbach H (1999) *Methods of theoretical physics*, vol 1–2. McGraw-Hill, Boston
15. Martin PA (2006) *Multiple scattering: interaction of time-harmonic waves with N obstacles*. Cambridge University Press, Cambridge
16. Kantorovich LV, Krylov VI (1964) *Approximate methods of higher analysis*. Interscience, New York
17. The Bateman Manuscript Project (1953) *Higher transcendental functions*, vol 1, 2. McGraw-Hill, New York
18. Gradshteyn IS, Ryzhik IM (2007) *Table of integrals, series, and products*. Academic Press, Amsterdam
19. Abramowitz M, Stegun IA (1972) *Handbook of mathematical functions*. National Bureau of Standards, Washington, DC
20. Polya G, Szegő G (1998) *Problems and theorems in analysis*, vol 1–2. Springer, New York
21. Titchmarsh EC (1962) *Eigenfunction expansions associated with second order differential equations*, part 1. Clarendon Press, Oxford
22. Hobson EW (2012) *The theory of spherical and ellipsoidal harmonics*. Cambridge University Press, Cambridge
23. Wainshtein LA, Belkina MG (1970) The method of double reduction, and infinite systems of linear equations for the expansion coefficients of the desired function with singularities. *Dokl USSR Acad Sci* 194(4):794–797 (in Russian)
24. Grinchenko VT, Luneva SA (1980) The sound field of shielded circular cylinder. *Acoust Phys* 26(3):462–466 (in Russian)
25. Smaryshev MD, Dobrovolskiy YuYu (1984) *Hydroacoustic antennas*. Sudostroenie, Leningrad (in Russian)
26. Vovk IV (1971) Sound excitation by transducer loaded on liquid wedge. *Acoust Phys* 17(2):311–314 (In Russian)